Monte Carlo simulation on dielectric and ferroelectric behaviors of relaxor ferroelectrics

X. Wang
Laboratory of Solid State Microstructures, Nanjing University, Nanjing 210093, People's Republic of China

J.-M. Liu[a)]
Laboratory of Solid State Microstructures, Nanjing University, Nanjing 210093, People's Republic of China; Department of Applied Physics, Hong Kong Polytechnic University, Hong Kong, People's Republic of China; and International Center for Materials Physics, Chinese Academy of Sciences, Shenyang, People's Republic of China

H. L. W. Chan and C. L. Choy
Laboratory of Solid State Microstructures, Nanjing University, Nanjing 210093, People's Republic of China and Department of Applied Physics, Hong Kong Polytechnic University, Hong Kong, People's Republic of China

(Received 2 October 2003; accepted 25 January 2004)

The dielectric and ferroelectric behaviors of relaxor ferroelectrics over the ferroelectric transition range are simulated using Monte Carlo simulation. The simulation is based on the Ginzburg–Landau ferroelectric model lattice in which a random distribution of two types of defects (dopants) which will suppress and enhance the local polarization, respectively, is assumed. The simulation reveals an evolution of the ferroelectric transitions from a normal first-order mode toward a diffusive mode, with increasing defect concentration. The simulated lattice configuration shows the microdipole ordered clusters embedded in the matrix of paraelectric phase over a wide range of temperature, a characteristic of relaxor ferroelectrics. The relaxor-like behaviors are confirmed by the lattice free energy, dielectric susceptibility, and ferroelectric relaxation evaluated as a function of the defect concentration. Finally, we present a qualitative comparison of our simulated results with the simulation based on the coarse-grain model [C. C. Su, B. Vugmeister, and A. G. Khachaturyan, J. Appl. Phys. **90**, 6345 (2001)]. © *2004 American Institute of Physics.*
[DOI: 10.1063/1.1686899]

I. INTRODUCTION

Relaxor ferroelectrics (RFs) represent a class of ferroelectric materials exhibiting abnormal dielectric and ferroelectric properties.[1,2] They show an excellent electromechanical performance and high dielectric susceptibility around the diffusive phase transition point, which are of special interest for sensor and transducer applications, while normal ferroelectrics (FEs) usually exhibit a sharp ferroelectric transition at a certain temperature. Structurally, it is believed that RFs are disordered electric-dipole media in which nanosized dipole ordered clusters are randomly embedded in the matrix of nonpolar phase (paraelectric phase, PE) below a certain temperature (typically 10^2 K).[3–19] A number of experimental and theoretical studies on the mechanism responsible for the abnormal polarization characteristics in RFs have been performed in the last several decades since the compositional inhomogeneity model proposed by Smolensky,[4] although a widely accepted physical portrait has not yet been available. The micromacro domain transition model,[3] the superparaelectric model,[5] the dipole-glass model,[6] the order–disorder model[7,8] and random-bond-random-field model,[9–11] among some other models are commonly employed to explain those experimentally observed effects for various RFs.[12–19]

In the comprehensive understanding of the microscopic characteristics of RFs, the concept of defect is basically important. It can also be viewed as a kind of compositional or structural inhomogeneity. As is well known, those mostly interested RFs are doped perovskite oxides in which special types of crystal defects are believed to be responsible for the observed relaxor behaviors.[2,14–19] These defects can be either impurity atoms distributed randomly in the lattice or off-center dopant ions which generate the so-called internal random fields or random bonds, or even a frustration of long-range ordering state due to some reasons.[2] Therefore, the local polarization may be suppressed or enhanced by these defects, depending on the types of interaction between these defects and the lattice. The role of these defects is considered in the theoretical models mentioned above in direct or indirect manner. For example, in the compositional inhomogeneity model, the defects may be impurity atom or dopant ion.[19] For the former, the impurity atoms in the lattice are viewed as disordered (random) static defects coupled locally with the transformational mode which is responsible for a stable dipole. Therefore, the defects may suppress the magnitude of local dipoles from site to site. For the latter, a model was

a)Author to whom correspondence should be addressed; electronic mail: liujm@nju.edu.cn

proposed by Vugmeister and Glinchuk[2] where a highly polarizable paraelectric host lattice with a displacive dielectric response to external electric field E is considered. If this lattice is doped by off-center dopants, a local dipole will form and the local dopant may occupy one of the crystallographically equivalent off-center sites around the unit cell center, and the resultant dipole moment may align along one of the equivalent vectors. Such an off-center displacement may lead to an enhancement of local dipole moment.

From the above picture on the role of defects in RFs, one may argue that RFs can be virtually viewed as originating from a random doping of the two types of defects into a normal FE lattice, although it could be difficult to clearly identify the type of doping which can certainly enhance or suppress the local polar moment. Quite a few models mentioned above are based on this argument and they introduced a random field into the polar interactions considered in the original models. Recently, this idea was once more adopted by Semenovskaya and Khachaturyan[20] in the Ginzburg–Landau thermodynamic description of the FE lattice with impurity-induced defects and subsequently by the same group in the coarse-grain description of the Ginzburg–Landau theory.[19] They included the effect of local dipole fluctuations induced by impurity ions and dopants in the Landau free energy. In addition, these models represent a realistic description of multi-domained FE lattice in which the dipole–dipole interaction, domain wall energy, and even long-range elastic energy are taken into account,[21–24] while these interactions have been less considered in other models. Therefore, it would be interesting to apply the Ginzburg–Landau model to study the dipole configuration, the dielectric and ferroelectric behaviors in a FE lattice doped with various defects. In a previous work, we employed this model to study the relaxation of dielectric and ferroelectric behaviors observed in ferroelectric copolymers irradiated by high-energy proton beams in which the irradiated sites were viewed as induced defects suppressing the local polarization.[25] The simulated results show a satisfactory consistency with the experiments.

In this article, we would like to perform a Monte Carlo (MC) simulation on the dipole configuration and dielectric behaviors in a defected Ginzburg–Landau model lattice in which both types of defects mentioned above are assumed to exist in a disordered configuration. We shall show a gradual evolution of the lattice from normal FE pattern to a coexistence of micropolar regions and nonpolar matrix. It is shown that the simulated dielectric susceptibility and polarization relaxation reproduce the main characteristics of RFs. We shall also perform a qualitative comparison of our simulated results with the simulation based on coarse-grain model of Su, Vugmeister, and Khachaturyan.[19]

II. MODEL AND ALGORITHM OF SIMULATION

A. Model

Our MC simulation starts from a two-dimensional (2D) $L\times L$ lattice with periodic boundary conditions, where the PE phase takes the square configuration and the FE phase the rectangular one. On each lattice site i an electric dipole (polar) is imposed with its moment vector $\mathbf{P}=(P_x,P_y)$, where P_x and P_y are the two components along x axis and y axis respectively, and their magnitude is allowed to change in order to minimize the lattice free energy. Although it was identified that for some RF systems the thermally activated flips of the dipoles may not be the unique mechanism with which the system undergoes the dielectric relaxation over the phase transition range, we still assume this mechanism to be the unique one because the other possible one, such as polarization resonance, cannot be dominant unless the temperature is low.[26] Furthermore, each moment vector $\boldsymbol{P}$ is limited to take four orientations $[0.\pm1]$ and $[\pm1.0]$ while its magnitude is allowed to take any value within (0.1). This limitation refers to the tetragonal structure of typical ferroelectric $BaTiO_3$.[23] It should be noted here that the coarse-grain model by Su and co-workers represents an updated description of the domain structure of RFs, and the extensive three-dimensional (3D) simulation based on this model indeed reveals the major features of RFs in terms of both microstructure and dielectric behaviors. Here in this article we give our attention to the configuration of electric dipoles in RFs. Although there is no quantitative comparison between our simulation and the 3D simulation,[19] a qualitative consistence between them will be revealed.

As proposed by Semenovskaya and Khachaturyan,[20] we consider several free energy terms which will determine the dipole configuration in the lattice. They include the Landau free energy, the dipole–dipole Coulomb interaction, and the gradient energy accounting for the domain wall inhomogeneity. For normal FEs, the long-range elastic interaction cannot be neglected, but it is not essential for RFs if one adopts the picture of microdipole ordered clusters embedded in the nonpolar matrix. For a dipole of moment $\boldsymbol{P}$ at site i in a 2D lattice, the Landau free energy can be written as

$$F_{\ell d}(P_i)=A_1(P_x^2+P_y^2)+A_{11}(P_x^4+P_y^4)+A_{12}P_x^2P_y^2 + A_{111}(P_x^6+P_y^6), \tag{1}$$

where subscript i refers to lattice site i, A_1, A_{11}, A_{12}, and A_{111} are the free energy coefficients, respectively. For normal FEs, $A_1>0$ favors a stable or metastable paraelectric phase while a first-order ferroelectric transition will occur if $A_1<0$.

The domain wall gradient energy for a site i and its neighbor j can be written as[20,23]

$$F_{gr}(P_{i,j})=\frac{1}{2}[G_{11}(P_{x,x}^2+P_{y,y}^2)+G_{12}P_{x,x}P_{y,y} + G_{44}(P_{x,y}+P_{y,x})^2+G'_{44}(P_{x,y}-P_{y,x})^2], \tag{2}$$

where $P_{i,j}=\partial P_i/\partial x_j$. Since parameters G_{11}, G_{12}, G_{44}, and G'_{44} are all positive, in most cases this free energy term is positive, favoring a uniformly parallel alignment of dipoles. In addition, a generic choice of G_{11}, G_{12}, G_{44}, and G'_{44} may

result in anisotropic domain wall energy. The dipole–dipole Coulomb interaction for site i and its neighbors j has the following form in the SI unit:[23]

$$F_{\mathrm{di}}(P_i)=\frac{1}{8\pi\varepsilon_0\chi}\sum_{\langle j\rangle}\left[\frac{P(r_i)\cdot P(r_j)}{|r_i-r_j|^3}-\frac{3[P(r_i)\cdot(r_i-r_j)][P(r_j)\cdot(r_i-r_j)]}{|r_i-r_j|^5}\right], \quad (3)$$

where ε_0 and χ are the vacuum susceptibility and relative dielectric susceptibility, respectively, $\langle j\rangle$ represents a summation over all sites within a separation radius R centered at site i, parameters r_i, r_j, $P(r_i)$ and $P(r_j)$ here should be vectors, r_i and r_j are the coordinates of sites i and j, respectively. In a strict sense, R should be infinite but an effective cutoff at $R=8$ is taken in our simulation without losing much accuracy. A minimization of F_{di} favors the head-to-tail alignment of dipoles. The energy for an antiparallel dipole alignment between two neighboring rows is slightly lower than that for a parallel alignment between the two rows. By an appropriate choice of parameters G_{11}, G_{12}, G_{44}, and G'_{44}, the system prefers a ferroelectric transition upon a lowering of temperature.

Finally, the electrostatic energy induced by an external electric field is

$$F_E(P_i)=-P_i\cdot E, \quad (4)$$

where E is the external electric field, and P_i and E are vectors. In our simulation, vector E takes the [1.0] direction. The total free energy counting all of these interactions for site i is

$$F_i(P_i)=F_{\ell\mathrm{d}}+F_{\mathrm{gr}}+F_{\mathrm{di}}+F_E. \quad (5)$$

Now we consider the effect of defects. It may be argued that a doping of these defects not only influences on the Landau free energy $F_{\ell\mathrm{d}}$ but also the other three terms F_{gr} and F_{di}. However, the latter two terms are related to the dipole–dipole interactions and then are the resultant effects. The randomly distributed defects lead to a spatial distribution for the coefficients A_1, A_{11}, A_{12}, and A_{111} in the Landau free energy Eq. (1). It was assumed that only A_1 is affected by the defects and the other three coefficients remain unchanged. That is[20]

$$A_1(r_i)=A_{10}+b_m\cdot C(r_i),\qquad A_{10}=\alpha(T-T_0),\quad \alpha>0, \quad (6)$$

where $\alpha>0$ is a materials constant, T is temperature, A_{10} is the coefficient A_1 in Eq. (1), T_0 is the critical temperature for a normal FE crystal with first-order phase transition features. Here we do not identify the difference between T_0 and the Curie point T_c because we do not focus on the critical phenomena associated with the FE transitions; $C(r)$ is the concentration of both types of defects, b_m is the coefficient characterizing the effect of defects on T_0, and it may be positive or negative, depending on the type of defects considered. We consider two types of defects: type I which can enhance the local dipole moment ($b_m<0$) and type II that will suppress the moment ($b_m>0$). We define a parameter C_p within [0.1] to partition the defects into the two types. There are totally $C_p\cdot C\cdot L^2$ type I defects and $(1-C_p)\cdot C\cdot L^2$ type II defects in the lattice.

B. Algorithm of simulation

As mentioned above, we assume that the dielectric and ferroelectric relaxation is uniquely determined by the thermally activated flip sequence. Thus the MC simulation is performed via the kinetic Metropolis algorithm. The simulation procedure is described below. For the initial lattice, each site is assigned a dipole with its moment magnitude P taken randomly within (0,1), and its orientation being one of the four states: $[\pm 1.0]$ and $[0.\pm 1]$, respectively. At the same time, whether a defect to be chosen to attach this site is determined by comparing a random number R_1 with C. If $R_1<C$, this site is attached with a defect and is not otherwise. Then second random number R_2 is generated to determine the type of this defect. If $R_2<C_p$, this defect belongs to type I, and to type II otherwise. The degree of order of both the moment enhancement and suppression is chosen randomly within $[0.5b_m, b_m]$.

The simulation begins at an extremely high temperature $kT=12.0$ where k is the Boltzmann constant and will be omitted later for convenience, and then T decreases step by step during the simulation ($T^0=3.0$ is chosen). At each temperature step, a site i is chosen at random, $F_{\ell\mathrm{d}}$, F_{gr}, F_{di}, and F_E are calculated, respectively, to obtain F_i. This site is then assigned another dipole with its magnitude and orientation taken randomly to simulate the dipole flip. Subsequently, F_i is calculated again to compare with the value of F_i before the assigned flip, and the difference of F_i after and before the assigned flip is ΔF_i. A probability p is calculated from the Metropolis algorithm

$$p=\exp(\Delta F_i/kT). \quad (7)$$

A third random number R_3 is generated and compared with p. If $R_3<p$, the assigned flip is performed and rejected otherwise. Then one cycle of simulation is completed and a new cycle is initiated until a given number of cycles has been completed. The time of simulation is scaled by the Monte Carlo step (mcs) and one mcs represents $L\times L$ cycles described above. In our simulation, the initial 600 mcs runs are done and then the configuration averaging is performed over the subsequent 2500 mcs. The lattice saved in the last run is chosen as the initial lattice for the next temperature step, and the simulation is done with the same algorithm. The data presented below represent an averaging over four runs with different seeds for random number generator.

For the thermally activated dipole flips, under an external ac-electric field E of frequency ω and amplitude E_0, the dielectric susceptibility χ is defined as[19]

$$\chi'=\frac{K}{NT}\left\langle\sum_i^N\frac{1}{1+(\omega\cdot\tau/\omega_0)^n}\right\rangle,\qquad \chi''=\frac{K}{NT}\left\langle\sum_i^N\frac{\omega\cdot\tau/\omega_0}{1+(\omega\cdot\tau/\omega_0)^n}\right\rangle, \quad (8)$$

TABLE I. System parameters used in the simulation.

Parameter	Value	Parameter	Value	Parameter	Value
T^0	3.0	α	1.0	A_{11}	−0.5
A_{12}	9.0	A_{111}	0.8	G_{11}	1.0
G_{14}	0.2	G_{44}	1.0	L	40
E_0	0.20	C_p	0.3	ω (mcs^{-1})	0.01

where $\langle\ \rangle$ represents the configuration averaging, n is the frequency dispersion exponent which depends on the system to be studied and we follow the Debye model and take $n=2$, χ' and χ'' are the real and imaginary parts of χ, ω_0 is the polariton frequency which is a material constant, τ is the averaged time for dipole switching from one state to another, $N=L^2$ and K is a temperature-dependent constant. For RFs, the lattice is inhomogeneous once $C>0$, time τ becomes site dependent and it can be expressed in the Arrhenius form[19]

$$\tau=\tau_0\cdot\tau'=\tau_{00}\exp(-F_{\ell d}/kT)\cdot\tau', \tag{9}$$

where τ_0 is the characteristic flip time for a noninteracting system, which is actually determined by the energy barrier referring to the Landau free energy $F_{\ell d}$ in the mean-field approximation, τ_{00} is the pre-exponential factor which scales the characteristic time for lattice vibration. If $F_{\ell d}<0$, it means that this dipole is in a stable state and its flip becomes relatively difficult. Here, $\tau_{00}=1.0$ and τ' is the averaged inversely number of flips for the dipole at site *i per mcs*. The free energy and lattice parameters used in the simulation are chosen and the dimensionless normalization of them is done following the work by Hu and Chen on the dynamics of domain switching in $BaTiO_3$ system.[23] Such a choice is somewhat arbitrary since we are not focusing on any realistic system in a quantitative sense. These parameters are given in Table I.

III. RESULTS OF SIMULATION AND DISCUSSION

A. Dipole configuration

We first study the evolution of the dipole configuration with increasing defect concentration C ($C_p=0.3$). In Fig. 1 we show the snapshot lattices for a normal FE lattice at several temperatures, where the length and direction of the arrows represent the magnitude and orientation of the dipole moment. For a high $T=5.0\gg T_0$, as shown in Fig. 1(a), the moment of all dipoles is very small and their alignment is totally disordered, a typical configuration for a paraelectric phase. As T is close to T_0 [$T=3.5$, Fig. 1(b)], the dipole moment is still small and no long-range dipole order is found, either.

Once T is below T_0, the ferroelectric phase transitions occur and the disordered dipole alignment evolves into a long-range ordered structure. A clear ferroelectric multidomain configuration is formed, with the well-predicted head-to-tail dipole alignment and preferred 90° domain walls, as shown in Fig. 1(c), where one sees the moment magnitude become much bigger than the PE phase. Those dipoles on the domain walls are still small in moment and their alignment remains partially disordered. At a low T ($T=1.0$), the degree of disordering on the walls is significantly suppressed and an almost perfect multi-domain lattice is observed.

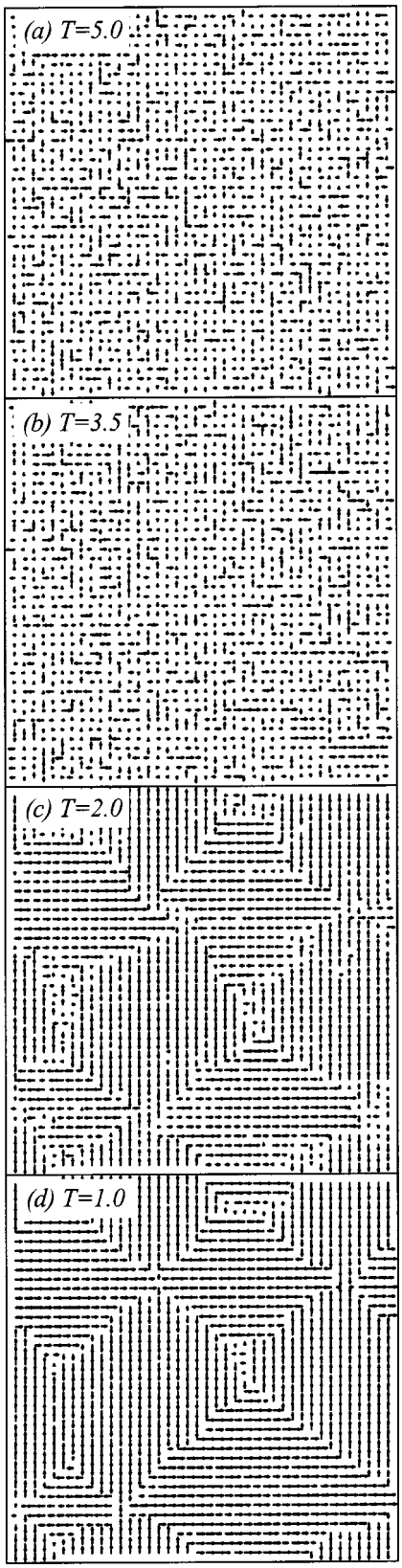

FIG. 1. Simulated snapshot dipole configuration at various temperatures (T) for a normal ferroelectric lattice.

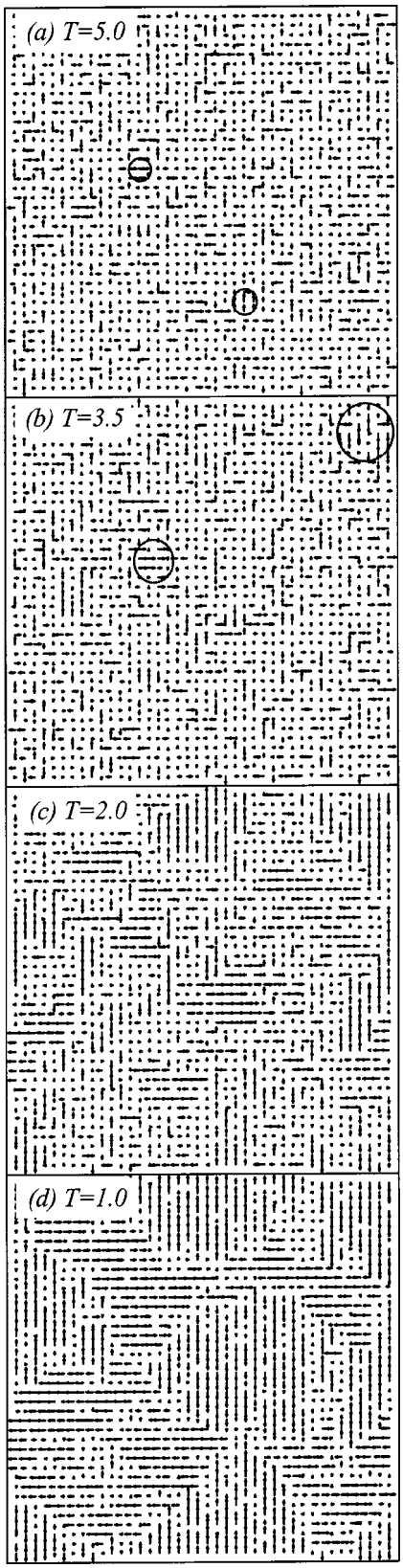

FIG. 2. Simulated snapshot dipole configuration at various temperatures (T) for a defective lattice of $C=0.5$. The circles indicate the local ordered dipole clusters.

When the defects are doped into the lattice ($C>0$), one sees quite different lattice configurations, as shown in Fig. 2 for $C=0.5$. Because the lattice is doped with two types of defects, we indeed find that there are some small-sized areas in which the dipole alignment is ordered at $T \gg T_0$ ($T=5.0$), i.e., some local clusters of ordered dipoles form at a temperature much higher than T_0. As $T=3.5$, slightly above T_0, this clustering tendency becomes more significant, as shown by the circled areas in Fig. 2(b). The number and size of the clusters increase with decreasing T. On the other hand, as T is below T_0, however, we do not see a perfect long-range ordered dipole configuration, while the lattice still consists of clustered areas of ordered dipoles embedded in the matrix of paraelectric phase. With further decreasing of T, a gradual growth and coalescence of these ordered clusters is observed, and a normal ferroelectric configuration can be predicted at a very low temperature.

Obviously, all features described above are well evidenced for RFs in which nanopolar clusters are embedded in the PE matrix over a wide range of temperature both above and below T_0. The feature of diffusive phase transitions is clearly reproduced, indicating that the present model works well in describing the microstructure of RFs. Here, it should be mentioned that in Fig. 2 the long-range ordered configuration is already well developed as T falls down to $T=1.0$ [Fig. 2(d)], at which the well-defined domain pattern can be identified although there still are some small dipole-disordered zones inside the domains. This configuration can be viewed as the frozen one, which reflects somehow the freezing behavior of relaxor ferroelectrics with decreasing temperature.[18] To further confirm this feature, we simulate the evolution of dipole configuration as $C=0.9$, as shown in Fig. 3. We can see that the FE phase transitions become even broader. While quite a number of relatively bigger dipole-ordered clusters can be seen at $T=5.0$ and 3.5, no well-defined domain is available even when T is as low as $T=1.0$. That is to say that when C is bigger, the ferroelectric transitions cannot be completed unless T is lower. Given the temperature, the bigger C is, the smaller the ordered clusters are.

B. Dielectric susceptibility

We present in Figs. 4(a) and 4(b) the evaluated dielectric susceptibility (real and imaginary parts χ' and χ'') as a function of T for lattices of different defect concentrations. Looking at the behaviors of the real part, the lattice at $C=0$ exhibits a typical FE transition characterized with the sharp peak of χ' at the transition point. Here it should be mentioned that the dielectric peak remains finite although the transition is first ordered, due to the limited lattice size and multi-domained structure. Correspondingly, the imaginary part also shows a peak at the transition point. With increasing defect concentration, one sees a remarkable broadening of the dielectric peak around the transition point and the peak position also shifts slightly toward the low-T side. Over the high temperature range ($T>T_0$), χ' decreases slightly with increasing C, while over the low T range ($T<T_0$) it increases significantly with C. This result may partially explain why the relaxor materials show a higher dielectric susceptibility than the normal FEs. The imaginary part χ'' does not show large C dependency over the high-T range, but it increases, too, with increasing C over the low-T range, the

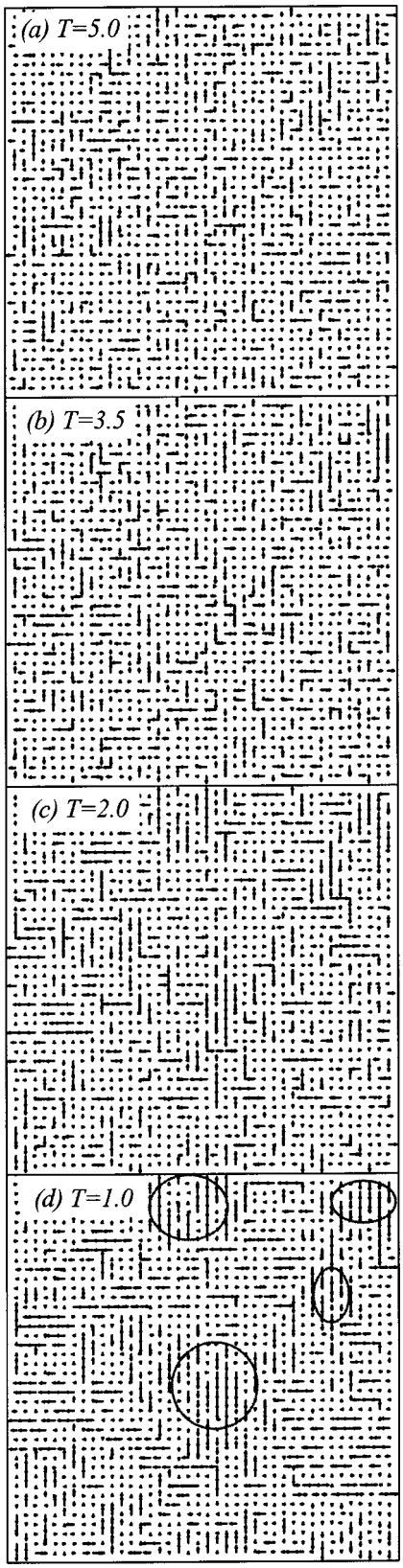

FIG. 3. Simulated snapshot dipole configuration at various temperatures (T) for a defective lattice of $C=0.9$. The circles indicate the local ordered dipole clusters.

more remarkable when T is lower. As C is extremely big ($C=0.9$), which means almost all lattice sites are occupied by the two types of defects, no peak for χ'' all around the transition point can be observed and it increases monotonously with decreasing temperature. This behavior has never been observed experimentally and its significance is under doubt (to be discussed below).

The significantly broadening behavior of χ' is the major characteristic of RFs whose microstructures are featured by the simulated configurations shown in Figs. 2 and 3. To understand the susceptibility enhancement at $T<T_0$, one may consult Eq. (8) and we focus on the real part χ'. It depends mainly on term $\tau_0 \sim \exp(-F_{\ell d}/kT)$ and τ'. For τ_0, given a temperature T, as the first-order approximation, one has $F_{\ell d} \sim [A_1 \cdot (T-T_0) + b_m \cdot C(1-2C_p)]P^2$ where $F_{\ell d}$ is the averaged value over the whole lattice. So $F_{\ell d}$ increases with increasing C and τ_0 becomes shorter as C is bigger. On the other hand, τ' would be shorter if a site is attached with a type II defect and longer for a type I defect. On the average sense, τ' becomes shorter since $C_p=0.3<0.5$. Therefore $(\tau_0 \cdot \tau')$ is smaller when C is bigger, resulting in larger χ' and χ'' when T is below T_0. When $T>T_0$, the energy barrier for dipole flip is zero and thus τ_0 can be viewed as a constant. However, those sites with the type I defects would need a longer time to realize the dipole flip because of the larger dipole moment P, thus τ' will become longer when C is bigger. Therefore, above T_0 one is shown a lower susceptibility for a lattice of bigger C.

For the diffusive phase transitions, the two parameters associated with the susceptibility peak, i.e., the peak position T_m and height χ'_m, as a function of the defect concentration C, is interesting. The evaluated T_m and χ'_m are presented in Fig. 4(c). Both parameters show a roughly linear decreasing with increasing C, indicating a significant suppression of the sharpness of the ferroelectric transition by the doped defects induced to the lattice.

C. Dynamic response of polarization

The excellent electromechanical performance of RFs is believed to originate from the flexible dynamic switching of the dipoles under external electric field, relative to the relatively worse dynamic response of the normal FEs of long-range dipole order.[27] We evaluate the static polarization component P_x of the lattice averaged over about 2500 periods of the ac-electric field and the results are presented in Fig. 5 where P_x is plotted as a function of temperature. With decreasing T, P_x increases gradually until $T \sim T_0$, and then begins to fall down when T is below T_0. This peak pattern reflects the strong fluctuations of ordering of the dipole moment during the phase transitions. What is interesting here is the dependence of P_x below the peak position on the defect concentration C. It is easily understood that for a normal FE of multi-domain structure, the residual polarization at low T under a small-signal field must be very close to zero, as shown in Fig. 5 as $C=0.0$. As C increases, one sees the residual polarization also increase and reach up to ~ 0.05 as $C=0.50$. This remarkable residual polarization allows us to argue that the microordered dipole clusters as shown in Figs. 2(c) and 2(d) are more flexible in responding to the external field than the long-range ordered domain shown in Figs. 1(c) and 1(d), because for the latter any dipole flip is seriously bonded by the dipole–dipole interaction and the domain wall

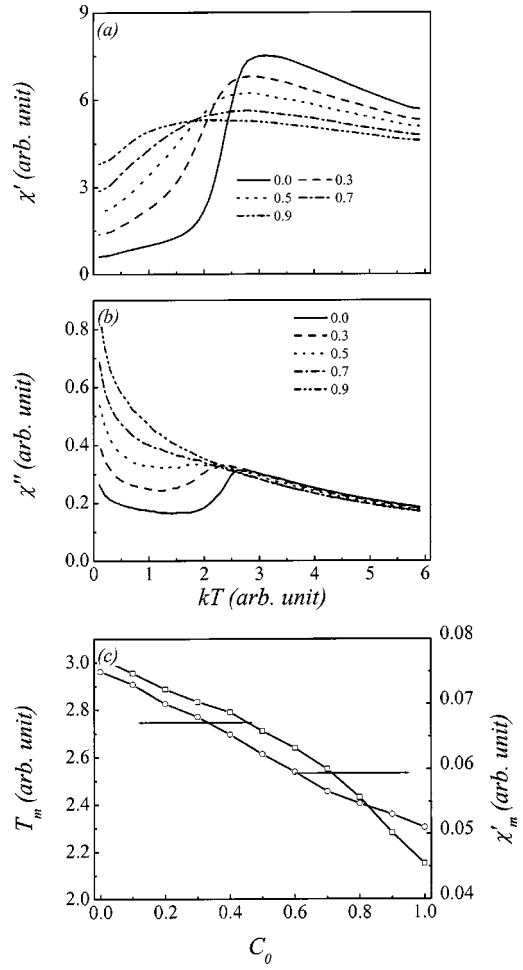

FIG. 4. Simulated dielectric susceptibility as a function of temperatures for lattices of different defect concentrations numerically labeled. (a) Real part χ' and (b) imaginary part χ''. (c) Evaluated temperature T_m for the dielectric susceptibility (χ') peak and the peak height χ'_m as a function of concentration C. The exponent $n=2$ is taken for the simulation [Eq. (8)].

energy, while for the former the clusters have no neighboring resistance on their boundaries.

As C is bigger, the volume fraction of the ordered dipole clusters becomes lower and thus the component P_x is smaller, too, because the averaging is over the whole lattice.

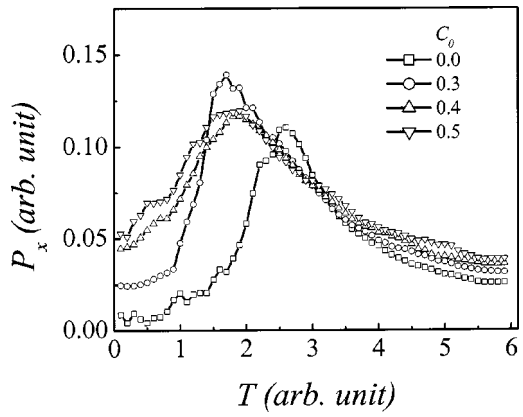

FIG. 5. Simulated polarization component P_x averaged over the whole lattice as a function of temperature T at different concentration C.

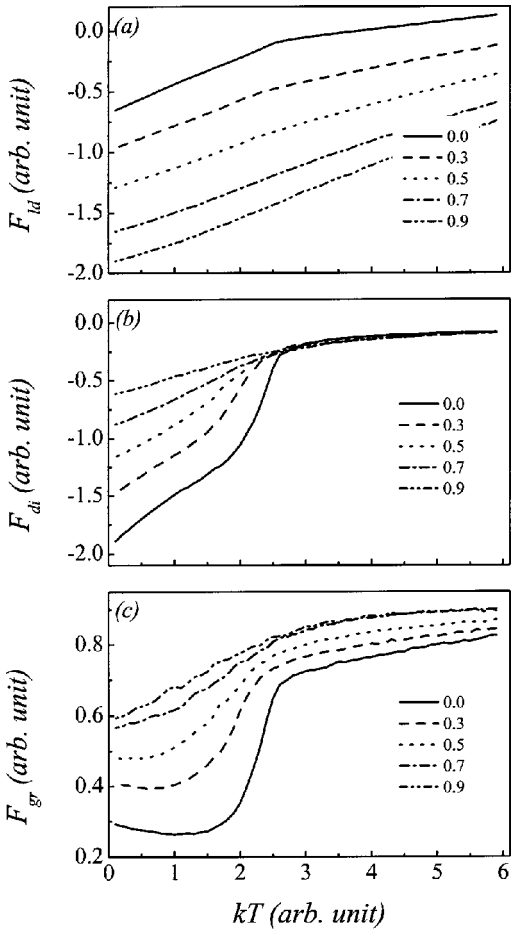

FIG. 6. Evaluated free energy terms $F_{\ell d}$, F_{di}, and F_{gr} as a function of temperature T for lattices of different concentration C.

The flexible dynamic response effect in RFs as revealed above can no longer be reflected by parameter P_x.

D. Dependence of free energy terms on defect concentration

We also study the free energy terms, $F_{\ell d}$, F_{di}, and F_{gr} as a function of T for the lattices of different values of C, and the results are shown in Fig. 6. It is shown that the behavior of $F_{\ell d}$ as a function of T can be divided into two regions: $T>T_0$ and $T<T_0$. In the two regions $F_{\ell d}$ changes linearly with T, with the slope at $T<T_0$ larger than that at $T>T_0$. The whole curve shifts downward with increasing C. The two well-separated regions at $C=0.0$ become hardly identifiable from each other with increasing C. To qualitatively understand these behaviors, we again look at Eq. (1). Because there are two types of defects doped into the lattice, as a rough approximation, we neglect the fourth-order and higher order terms and write $F_{\ell d}$ as

$$\begin{aligned} F_{\ell d} &\approx \alpha P_2^2 T + [|b_m| \cdot C(1-C_p) - \alpha T_0] P_2^2 + \alpha P_1^2 T \\ &\quad - (|b_m| \cdot C \cdot C_p + \alpha T_0) P_1^2 \\ &\approx \alpha P_1^2 T - (|b_m| \cdot C \cdot C_p + \alpha T_0) P_1^2, \end{aligned} \tag{10}$$

where P_1 and P_2 are the averaged dipole moment for those sites doped with type I and type II defects, respectively. Ob-

viously, $P_1 \gg P_2 \sim 0.0$. It is clearly seen that $F_{\ell d}$ is a linear function of T as long as P_1 does not change much. In fact, in the case of $C=0$, except from the transition point T_0 which is site dependent in the case of $C>0$, P_1 does not change remarkably above and below T_0, respectively, but at $T<T_0$ it is larger than that at $T>T_0$, thus the slope of $F_{\ell d}(T)$ at $T<T_0$ is, of course, bigger than that at $T>T_0$. As $C>0$, the change of P is gradual over a wide range of temperature and the two linear regions at $C=0$ are smeared gradually, too. As for the downshift of the $F_{\ell d}-T$ curve, Eq. (10) shows that the increasing C results in this effect, and basically, one can predict a linear dependence of the shift on C.

The behaviors of terms F_{di} and F_{gr} as a function of T as various values of C, shown in Figs. 6(b) and 6(c), are easily understood. For F_{di}, we look at the dependence on C below T_0, as shown in Fig. 6(b). Take the case of $C=0$ as a reference. Once the FE transition occurs, the dipole ordering leads to a rapid decrease of F_{di}. The introduction of the defects gives rise to the disordering of the dipole alignment on the one hand, and a slight reduction of the dipole moment on the other. Both effects will increase F_{di}. At $C=0.9$, one cannot observe the transition anymore.

For the gradient energy F_{gr}, it is always positive and its magnitude is determined by the degree of disorder of dipole alignment, i.e., the difference in moment and orientation between site i and its four neighbors. The very weak dipole ordering sequence above T_0 with decreasing T is reflected by the decreasing of F_{gr} with decreasing T, as shown in Fig. 6(c). As C increases, the very small averaged dipole moment above T_0 is enhanced due to $C_p=0.3$, leading to a slight upward shift of F_{gr}. At $C=0$, the rapid decrease of F_{gr} at a temperature slightly below T_0 is ascribed to the ferroelectric transition where P_{ij} in Eq. (3) is sharply reduced due to the first-order dipole ordering. This effect will be weakened by the introduced defects, since the defect-induced inhomogeneity enhances P_{ij}. Thus, F_{gr} increases with increasing C.

IV. COMPARISON AND REMARKS

As mentioned above, the extensive MC simulation in a 3D lattice based on the coarse-grain model by Su and co-workers[19] reproduced quite well the major features of RFs. A qualitative consistency of our simulation with the coarse-grain model simulation is identified. In terms of the microstructure of RFs, both simulations reveal a picture of ferroelectric nano-sized polar-ordered regions embedded in the matrix of paraelectric phase due to the defect effect. The gradual or ''diffuse'' phase transition feature when C increases is revealed in both simulations. Our simulation started from a disordered dipole configuration, which produces a nonzero but very small average macroscopic dipole moment for lattices of different C at low T range, as shown in Fig. 5, which coincides with the simulation of Su and co-workers[19] while the peaks appearing during the phase transitions in Fig. 5 are induced by the small ac-electric field. In fact, from the dipole configurations shown in Figs. 1–3, it is shown that each dipole in the ordered clusters increases in magnitude with decreasing temperature, although the lattice averaged dipole moment remains quite small even at low T. The freezing effect of the dipole flip at low T is also identified if one refers to the dipole configurations shown in Figs. 1–3. We did not simulate the configuration evolution from an ordered initial lattice, but it can be predicted that such a simulation will produce similar results as revealed in the coarse-grain model.

Furthermore, looking at the dielectric constant as a function of T, one is shown that the coarse-model of Su and co-workers[19] reveals a diffusive frequency dispersion of the dielectric constant for RFs in comparison with normal ferroelectrics. This diffusing frequency dispersion behavior can be indirectly reflected in our simulated results shown in Figs. 4 and 5, where the significantly broadening dielectric constant [Fig. 4(a)] and dipole moment P_x (Fig. 5) as a function of temperature, with increasing defect concentration C, are indicated. Therefore, we are shown that our simulation is qualitatively consistent with the coarse-grain model and the associated MC simulation.[19]

The main properties of RFs have been reproduced as shown above by using the Ginzburg–Landau model for a defective lattice. We are shown that this model reproduces the coexistence of the microdipole-ordered regions and PE phase, and the diffusive phase transition behaviors for dielectric susceptibility and domain switching as well. Compared to other models for RFs, the Ginzburg–Landau model represents one of the realistic descriptions of FE phase transitions. It takes into account the main interactions for ferroelectric systems. In fact, this model has been very successful in describing the details of 90° and 180° domain structures which represent the most complicated issue in the physics of ferroelectrics. Therefore, together with the work of Semenovskaya and Khachaturyan, the present investigation is an important extension of the Ginzburg–Landau model to the relaxor ferroelectrics.

However, it is still too early to claim a realistic and quantitative calculation of the dielectric and ferroelectric properties for real RFs using this model and associated simulation algorithms. The main challenges can be summarized as follows. First, the significant frequency dependence of the dielectric susceptibility for RFs cannot be reasonably reproduced by this model, although this inconsistence may be ascribed to the definition of the susceptibility Eq. (8) which is based on unique characteristic time for dielectric relaxation, as assumed in the Debye model. The frequency dispersion of dielectric susceptibility of RFs was extensively studied experimentally and different models were proposed for different RFs. In fact, with the definition Eq. (8) where $n=2$, the simulated frequency dispersion is much more significant than that experimentally revealed.[28] Second, the Ginzburg–Landau model assumes that the thermally activated dipole flip is the unique mechanism for the dielectric relaxation. This assumption was recently criticized and it was claimed that the low temperature resonance response is important for the dielectric relaxation in the dipole-ordered regions.[26] Third, one may argue that the four allowed states of the dipole orientation as imposed over the whole temperature range is not reasonable. For the long-range ordered state well below T_0 in the rectangle lattice, this assumption is acceptable, while the number of allowed states may be more than

four above T_0 and during the phase transitions. A bigger number of states will result in a higher dielectric susceptibility because parameter τ' is shorter. Finally, the disorder–order phenomenon as often identified for the typical RFs cannot be predicted by the present model. The essence of this effect seems still unclear in the framework of the Ginzburg–Landau model. These issues are studied in the ongoing work and will be reported elsewhere.

V. CONCLUSION

In conclusion, we have investigated in detail the dielectric and ferroelectric relaxation of a mode relaxor system doped with two types of defects by Monte Carlo simulation technique. The mode lattice is based on the Ginzburg–Landau model of first-order phase transitions and the two types of defects are assumed to play a role of enhancing and suppressing the local dipole moment, respectively. It has been revealed that with increasing defect concentration the simulated dipole configuration evolves from the normal ferroelectric lattice to the relaxor ferroelectric one in which the microregions of ordered-dipole clusters are embedded in the matrix of paraelectric phase. The simulated dielectric susceptibility as a function of temperature shows significantly diffusive characters and its value in the ferroelectric ordering state increases with the increasing defect concentration. The flexible dynamic response of the dipoles to the external ac-electric field with the normal ferroelectrics as reference has been demonstrated. A qualitative consistency between the present simulation and the coarse-grain model simulation is shown.

ACKNOWLEDGMENTS

The authors would like to acknowledge the support from the National Key Project for Basic Research of China (2002CB613303), the National Natural Science Foundation of China through Project Nos. 50332020 and 50172020, and LSSMS of Nanjing University as well.

[1] L. E. Cross, Ferroelectrics **151**, 305 (1994).
[2] B. E. Vugmeister and M. D. Glinchuk, Rev. Mod. Phys. **62**, 993 (1990).
[3] X. Yao, Z. Chen, and L. E. Cross, J. Appl. Phys. **54**, 3399 (1983).
[4] G. A. Smolensky, J. Phys. Soc. Jpn. **28**, 26 (1970).
[5] L. E. Cross, Ferroelectrics **76**, 241 (1987).
[6] D. Viehland, S. J. Jang, L. E. Cross, and M. Witting, J. Appl. Phys. **68**, 2916 (1990).
[7] N. Setter and L. E. Cross, J. Mater. Sci. **15**, 2478 (1982).
[8] C. A. Randall and A. S. Bhalla, Jpn. J. Appl. Phys., Part 1 **29**, 327 (1990).
[9] V. Westphal, W. Kleemann, and M. D. Glinchuk, Phys. Rev. Lett. **68**, 847 (1992).
[10] W. Kleemann, Int. J. Mod. Phys. B **7**, 2469 (1993).
[11] R. Pirc, B. Tadic, and R. Blinc, Phys. Rev. B **36**, 8607 (1987).
[12] A. P. Levanyuk and A. S. Sigov, *Defects and Structural Phase Transitions* (Gordon and Breach, New York, 1988).
[13] N. Ichinose, Ferroelectrics **203**, 187 (1997).
[14] Q. M. Zhang, J. Zhao, T. R. Shrout, and L. E. Cross, J. Mater. Res. **12**, 1777 (1997).
[15] C. H. Park and D. J. Chadi, Phys. Rev. B **57**, 13961 (1998).
[16] Z. Wu, W. Duan, Y. Wang, B. L. Gu, and X. W. Zhang, Phys. Rev. B **67**, 052101 (2003).
[17] E. Courtens, Phys. Rev. Lett. **52**, 69 (1984).
[18] A. K. Tagantsev, Phys. Rev. Lett. **72**, 1100 (1994).
[19] C. C. Su, B. Vugmeister, and A. G. Khachaturyan, J. Appl. Phys. **90**, 6345 (2001).
[20] S. Semenovskaya and A. G. Khachaturyan, J. Appl. Phys. **83**, 5125 (1998).
[21] W. Cao and L. E. Cross, Phys. Rev. B **44**, 5 (1991).
[22] S. Nambu and D. A. Sagala, Phys. Rev. B **50**, 5838 (1994).
[23] H. L. Hu and L. Q. Chen, Mater. Sci. Eng., A **238**, 182 (1997).
[24] B. G. Potter, Jr., V. Tikare, and B. A. Tuttle, J. Appl. Phys. **87**, 4415 (2000).
[25] J.-M. Liu, S. T. Lau, H. L. W. Chan, and C. L. Choy (unpublished).
[26] Z. Y. Cheng, R. S. Katiyar, X. Yao, and A. S. Bhalla, Phys. Rev. B **57**, 8166 (1998).
[27] V. A. Isupov and E. P. Smirnova, Ferroelectrics **90**, 141 (1989).
[28] A. K. Jonscher, *Dielectric Relaxation in Solids* (Chelsea Dielectrics, London, 1983).